

$D^0 \rightarrow \pi^+ \pi^- \pi^+ \pi^-$, $D^0 \rightarrow K^+ K^- \pi^+ \pi^-$ amplitude analyses and properties of $a_1(1260)$, $\pi(1300)$, $a_1(1640)$

P. d'Argent^a, N. Skidmore^{*b}, J. Benton,^b J. Dalseno,^b E. Gersabeck,^a S.T. Harnew,^b P. Naik,^b C. Prouve^b and J. Rademacker^b

^b*H.H. Wills Physics Laboratory, University of Bristol*

^a*Physikalisches Institut, Ruprecht-Karls-Universität Heidelberg*

E-mail: p.dargent@cern.ch, nicola.skidmore@cern.ch,
jack.b.benton@gmail.com, J.Dalseno@bristol.ac.uk,
evelina.gersabeck@cern.ch, sam.harnew@bristol.ac.uk,
paras.naik@bristol.ac.uk, claire.prouve@cern.ch,
jonas.rademacker@bristol.ac.uk

The resonant substructures of $D^0 \rightarrow \pi^+ \pi^- \pi^+ \pi^-$ and $D^0 \rightarrow K^+ K^- \pi^+ \pi^-$ decays are studied using data collected by the CLEO detector. Amplitude analyses are performed using a data driven regularization procedure to limit the model complexity. For the $D^0 \rightarrow \pi^+ \pi^- \pi^+ \pi^-$ decay the prominent contributions are the decay modes $D^0 \rightarrow a_1(1260)^+ \pi^-$, $D^0 \rightarrow \sigma f_0(1370)$ and $D^0 \rightarrow \rho(770)^0 \rho(770)^0$. The broad resonances $a_1(1260)^+$, $\pi(1300)^+$ and $a_1(1640)^+$ are studied in detail, including quasi-model-independent parametrizations of their lineshapes.

The amplitude analysis of $D^0 \rightarrow K^+ K^- \pi^+ \pi^-$ decays uses a significantly improved formalism with respect to previous analyses of the decay. The largest contributions to the decay are found to be the decay modes $D^0 \rightarrow \phi(1020) \rho(770)^0$, $D^0 \rightarrow K_1(1270)^+ K^-$ and $D^0 \rightarrow K(1400)^+ K^-$. A search for CP asymmetries at both global and amplitude component level yield no evidence for CP violation in either decay mode.

The work presented here is published in Ref. [1].

*XVII International Conference on Hadron Spectroscopy and Structure
25-29 September, 2017
University of Salamanca, Salamanca, Spain*

*Speaker.

1. Introduction

We present the amplitude analyses of $D^0 \rightarrow \pi^+\pi^-\pi^+\pi^-$ and $D^0 \rightarrow K^+K^-\pi^+\pi^-$ decays performed using data from the CLEO experiment. These four-body decay modes have a rich resonant structure and the potential to make important contributions to the determination of the CP -violating phase γ from $B^- \rightarrow DK^-$ and related decays through both model dependent and model independent methods [2, 3, 4, 5, 6, 7]. Previously, the FOCUS experiment has performed amplitude analyses of both $D^0 \rightarrow \pi^+\pi^-\pi^+\pi^-$ and $D^0 \rightarrow K^+K^-\pi^+\pi^-$ decays [8, 9] albeit with limited statistics. Most recently CLEO has performed an amplitude analysis of the $D^0 \rightarrow K^+K^-\pi^+\pi^-$ decay [10], however both the amplitude analysis formalism and the analysis software used has undergone significant development, motivating re-analysing the CLEO data. The work presented here is published in Ref. [1].

2. Datasets and selection

The datasets used for these analyses were produced through symmetric e^+e^- collisions at CESR from 1995 to 2008. CLEO collected these data using three different detector configurations: CLEO II.V, CLEO III and CLEO-c. All datasets utilise flavour tagging to determine the flavour of the signal D decay. Data collected at collision energies consistent with the $\psi(3770)$ resonance ($\sqrt{s} = 3770\text{MeV}$) also allows for events to be CP tagged, whereby the CP state of the signal D decay can be determined if the other D meson in the event is reconstructed in a state of definite CP .

A peaking background present in both analyses is $D^0 \rightarrow K_S^0(\rightarrow \pi^+\pi^-)h^+h^-$ decays. Despite having the same final state as the signal decay the relatively long lifetime of the K_S^0 meson means that it is an incoherent process. Both analyses use a mass veto which is applied to the invariant mass spectrum of $\pi^+\pi^-$ combinations to remove these events from the data samples.

3. Formalism

The total amplitude for a four-body decay $D^0 \rightarrow h_1 h_2 h_3 h_4$ is given by the coherent sum over all intermediate state amplitudes $A_i(\mathbf{x})$, each weighted by a complex coefficient $a_i = |a_i|e^{i\phi_i}$ that is to be measured from data,

$$A_{D^0}(\mathbf{x}) = \sum_i a_i A_i(\mathbf{x}). \quad (3.1)$$

We use the isobar approach to construct $A_i(\mathbf{x})$, which assumes that the four-body decay process can be factorized into subsequent two-body decay amplitudes [11, 12, 13]. This gives rise to quasi-2-body decays of the form $D^0 \rightarrow (R_1 \rightarrow h_1 h_2)(R_2 \rightarrow h_3 h_4)$ and cascade decays of the form $D^0 \rightarrow h_1 [R_1 \rightarrow h_2 (R_2 \rightarrow h_3 h_4)]$. The intermediate state amplitudes, $A_i(\mathbf{x})$, are parameterized as a product of form factors, B_L , which are taken as the Blatt-Weisskopf penetration factors [14], Breit-Wigner propagators, T_R , which are included for each resonance R , and an overall angular distribution, S , constructed using the covariant Zemach tensor formalism [15, 16, 17]

$$A_i(\mathbf{x}) = B_{L_D}(\mathbf{x}) [B_{L_{R_1}}(\mathbf{x}) T_{R_1}(\mathbf{x})] [B_{L_{R_2}}(\mathbf{x}) T_{R_2}(\mathbf{x})] S_i(\mathbf{x}). \quad (3.2)$$

We employ an improved lineshape description for resonant particles decaying to three-body final states as is in the case for cascade decays. Here, the energy dependent width of the resonant particle

is determined from the resonant substructure of the three-body amplitude. The total amplitude, $A_{D^0}(\mathbf{x})$, is used to form a probability density function (PDF) that also incorporates the contributions from background. Efficiency effects across phase space are accounted for through the use of a detector-simulated Monte Carlo integration technique.

4. Amplitude model fit

Both analyses use a data-driven regularisation method known as the Least Absolute Shrinkage and Selection Operator (LASSO) [18, 19] to determine which of the many possible amplitude contributions to include in the amplitude model, balancing improvement in the fit quality with increased model complexity. It should be noted that there are groups of amplitude components possessing the same angular structure that can produce artificially high interference effects among each other. For these components, alternative amplitude models consider each contribution separately. A binned χ^2 measure is used to determine the quality of the fit in the five-dimensional phase space,

$$\chi^2 = \sum_{b=1}^{N_{\text{bins}}} \frac{(N_b - N_b^{\text{exp}})^2}{N_b^{\text{exp}}}, \quad (4.1)$$

where N_b is the number of data events in bin b , N_b^{exp} is the number of events predicted by the fitted PDF in bin b and N_{bins} is the number of bins. An adaptive binning scheme [10] is used to ensure there are sufficient statistics in each bin. We quote χ^2 divided by the effective number of degrees of freedom, ν . For the $D^0 \rightarrow \pi^+\pi^-\pi^+\pi^-$ fit $\nu = (N_{\text{bins}} - 1) - N_{\text{par}}$ and for the lower statistics $D^0 \rightarrow K^+K^-\pi^+\pi^-$ channel, ν is determined using a pseudo-experiment technique.

5. $D^0 \rightarrow \pi^+\pi^-\pi^+\pi^-$ amplitude analysis results

The fit to $D^0 \rightarrow \pi^+\pi^-\pi^+\pi^-$ data yields $\chi^2/\nu = 1.40$ where $\nu = 221$ and figure 1 shows the distributions of selected phase space observables demonstrating good agreement between the data and the fit model. The dominant contribution is the $a_1(1260)$ resonance in the decay modes $a_1(1260) \rightarrow \rho(770)^0\pi$ and $a_1(1260) \rightarrow \sigma\pi$ followed by the quasi-two-body decays $D \rightarrow \sigma f_0(1370)$ and $D \rightarrow \rho(770)^0\rho(770)^0$. We find that the decay $D^0 \rightarrow a_1(1260)^+\pi^-$ dominates over $D^0 \rightarrow a_1(1260)^-\pi^+$, which is similar to the pattern observed in the B sector, where $B^0 \rightarrow a_1(1260)^+\pi^-$ is preferred over $B^0 \rightarrow a_1(1260)^-\pi^+$ [20, 21]. Resonance properties of the $a_1(1640)^+$, $a_1(1260)^+$ and $\pi(1300)^+$ were also determined from the fit to data and are given in table 1. We verify the $a_1(1640)^+$, $a_1(1260)^+$ and $\pi(1300)^+$ resonant phase motion in a quasi-model-independent way [22]. The Breit-Wigner lineshape is replaced by a complex-valued cubic spline. The interpolated cubic spline has to pass through independent complex knots spaced in the $m^2(\pi^+\pi^+\pi^-)$ region around the nominal mass. Figure 2 shows these interpolated splines with the expectation from a Breit-Wigner shape with the mass and width from the nominal fit superimposed taking into account the (statistical) uncertainties on the mass and width. The interpolated splines generally reproduce the features of the Breit-Wigner parametrization with the resulting Argand diagrams showing a circular, counter-clockwise trajectory which is the expected behavior of a resonance.

Table 1: Resonance parameters determined from the fit to $D^0 \rightarrow \pi^+ \pi^- \pi^+ \pi^-$ decays. The uncertainties are statistical, systematic and model-dependent, respectively.

Parameter	Value
$m_{a_1(1260)}$ (MeV/ c^2)	$1225 \pm 9 \pm 17 \pm 10$
$\Gamma_{a_1(1260)}$ (MeV)	$430 \pm 24 \pm 25 \pm 18$
$m_{\pi(1300)}$ (MeV/ c^2)	$1128 \pm 26 \pm 59 \pm 37$
$\Gamma_{\pi(1300)}$ (MeV)	$314 \pm 39 \pm 61 \pm 26$
$m_{a_1(1640)}$ (MeV/ c^2)	$1691 \pm 18 \pm 16 \pm 25$
$\Gamma_{a_1(1640)}$ (MeV)	$171 \pm 33 \pm 20 \pm 35$

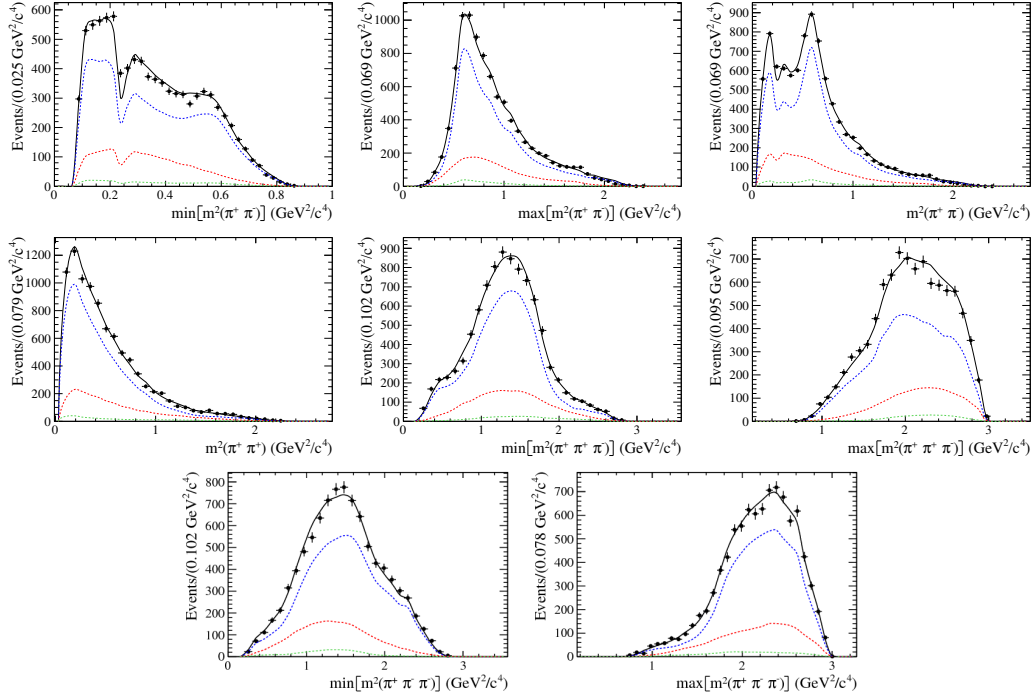


Figure 1: Invariant mass distributions of $D^0 \rightarrow \pi^+ \pi^- \pi^+ \pi^-$ signal candidates (points with error bars) and fit projections (black solid line). The signal component is shown in blue (dashed), the background component in red (dashed) and the mis-tagged contribution in green (dashed). The effect of the K_S^0 veto can clearly be seen in the top left projection.

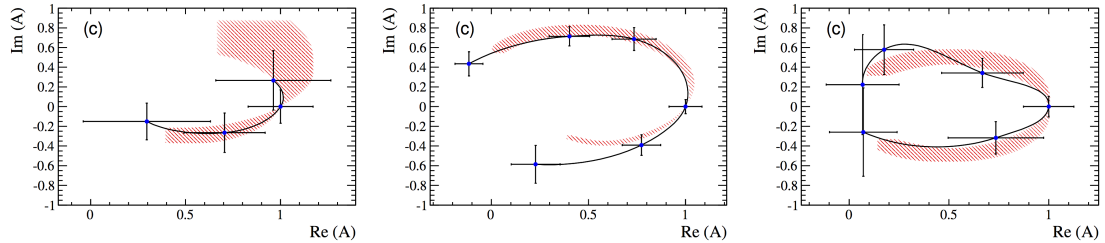


Figure 2: Argand diagram of the quasi-model-independent $a_1(1640)$, $a_1(1260)$ and $\pi(1300)$ lineshapes. The fitted knots are displayed as points with error bars and the black line shows the interpolated spline. The Breit-Wigner lineshape with the mass and width from the nominal fit is superimposed (red area). The latter is chosen to agree with the interpolated spline at the point $\Re(A) = 1$, $\Im(A) = 0$.

6. $D^0 \rightarrow K^+ K^- \pi^+ \pi^-$ amplitude analysis results

The fit to $D^0 \rightarrow K^+ K^- \pi^+ \pi^-$ data yields a χ^2/ν value of 1.5 where $\nu = 116$. Figure 3 shows the distributions of selected phase space observables, which demonstrate reasonable agreement between data and the fit model. Relative to the previous analysis performed on the same data set [10], the most notable difference is the fit fraction of the $\phi(1020)\rho(770)^0$ S -wave due to our modified description of the VV D -wave. In Ref. [10], the component labeled as D -wave is a superposition of D and S waves which led to a large interference between the components labeled as S wave and D wave. In this analysis, we parametrize a pure D -wave and find an interference fraction between the $\phi(1020)\rho(770)^0$ S - and D -waves of -3.7% . Taking these interference fractions into account, the combined $\phi(1020)\rho(770)^0$ S - and D -wave fraction is consistent between both analyses. The largest differences in our results are in the cascade topology due to the significant improvement in the description of the lineshapes of resonance decays to three-body final states. We also find that the process $D^0 \rightarrow K^{**+} K^-$, where K^{**} represents any excited kaon, dominates over $D^0 \rightarrow K^{*-} K^+$. We also observe a significant $K(1270) \rightarrow K^*(1430) \pi$ component in agreement with Ref. [9] but not with Ref. [10]. The description of this type of decay chain, with a daughter whose mean mass is outside the kinematically allowed region, benefits particularly from our improved lineshapes.

For both amplitude analyses CP asymmetries are investigated at both a global and amplitude component level, no evidence for CP violation is seen.

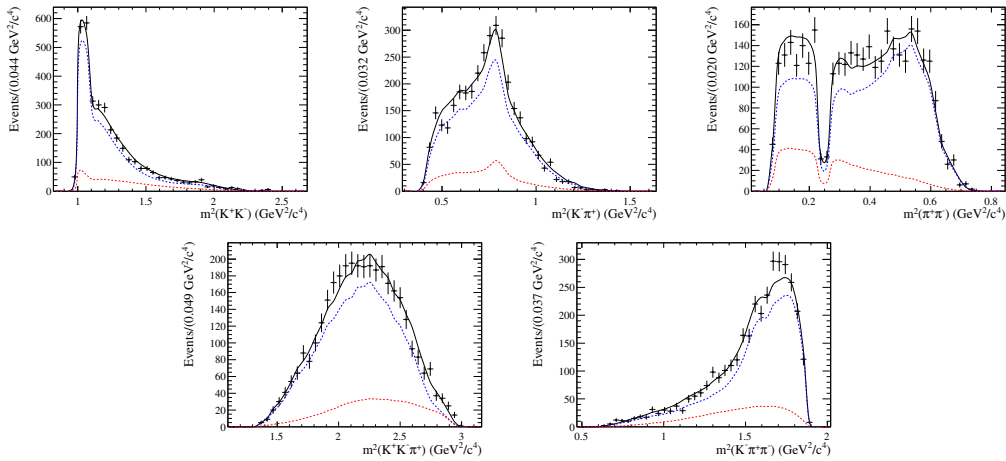


Figure 3: Invariant mass distributions of $D^0 \rightarrow K^+ K^- \pi^+ \pi^-$ signal candidates shown as points with error bars. The overall fit projection is shown in black, the signal in blue and the background in red. The effect of the K_S^0 veto can clearly be seen in the $m^2(\pi^+ \pi^-)$ projection.

7. Conclusion

Amplitude analyses of both $D^0 \rightarrow \pi^+ \pi^- \pi^+ \pi^-$ and $D \rightarrow K^+ K^- \pi^+ \pi^-$ decays have been performed using data collected by the CLEO detector. A data driven model-building procedure has been applied which balances the fit quality against the number of free fit parameters. No CP violation is seen for either channel. In addition to shedding light on the dynamics of $D^0 \rightarrow h^+ h^- \pi^+ \pi^-$ decays, these results are expected to provide important input for a determination of the CP -violating phase γ in $B^- \rightarrow DK^-$ decays.

Acknowledgments

This analysis was performed using CLEO data. The authors of these proceedings (some of whom were members of CLEO) are grateful to the collaboration for the privilege of using these data. We also gratefully acknowledge the support of the UK Science and Technology Facilities Council, the European Research Council 7 / ERC Grant Agreement number 307737 and the German Federal Ministry of Education and Research (BMBF).

References

- [1] d'Argent, P., Skidmore, N., Benton, J., Dalseno, J., Gersabeck E., Harnew, S. T., Naik, P., Prouve, C., Rademacker, J. *Amplitude analyses of $D^0 \rightarrow \pi\pi\pi\pi$ and $D^0 \rightarrow K^+K^-\pi^+\pi^-$* *Journal of High Energy Physics* **143** (2072)
- [2] Gronau, M., Wyler, D. *On determining a weak phase from CP asymmetries in charged B decays* *Phys.Lett.* **B265** (172-176) (1991)
- [3] Gronau, M., London, D. *How to determine all the angles of the unitarity triangle from $B_d \rightarrow DK_s$ and $B_s^0 \rightarrow D\phi$* *Phys.Lett.* **B253** (483-488) (1991)
- [4] Atwood, D., Dunietz, I., Soni, A. *Enhanced CP violation with $B \rightarrow KD^0(\bar{D}^0)$ modes and extraction of the Cabibbo-Kobayashi-Maskawa Angle γ* *Phys.Rev.Lett.* **78** (3257-3260) (1997)
- [5] Giri, A., Grossman, Y., Soffer, A., Zupan, J. *Phys. Rev. D* **68** (054018) (2003) *Determining γ using $B^\pm \rightarrow DK^\pm$ with multibody D decays*
- [6] Belle collaboration *Measurement of ϕ_3 with Dalitz plot analysis of $B^\pm \rightarrow D^{(*)}K^\pm$ decays* *Phys. Rev. D* **70** (072003) (2004)
- [7] Rademacker, J., Wilkinson, G. *Determining the unitarity triangle γ with a four-body amplitude analysis of $B^\pm \rightarrow (K^+K^-\pi^+\pi^-)_D K^\pm$ decays* *Phys.Lett.* **B647** (400-404) (2007)
- [8] FOCUS Collaboration, *Study of the $D^0 \rightarrow \pi^-\pi^+\pi^-\pi^+$ decay*, *Phys.Rev.* **D75** (052003) (2007)
- [9] FOCUS Collaboration, *Study of the $D^0 \rightarrow K^+K^-\pi^+\pi^-$ decay*, *Phys. Lett.* **B610** (225-234) (2005)
- [10] CLEO Collaboration, *Amplitude analysis of $D^0 \rightarrow K^+K^-\pi^+\pi^-$* , *Phys.Rev.* **D85** (122002) (2012)
- [11] Mandelstam, S., Paton, J.E., Peierls, R., Sarker, A. *Isobar approximation of production processes* *Annals of Physics* **18** (198 - 225) (1962)
- [12] Herndon, D., Söding, P., Cashmore, R. *Generalized isobar model formalism* *Phys. Rev. D* **11** (3165-3182) (1975)

- [13] Brehm, J.J. *Unitarity and the isobar model: Two-body discontinuities* *Annals of Physics* **108** (454 - 476) (1977)
- [14] von Hippel, F., Quigg, C. *Centrifugal-Barrier Effects in Resonance Partial Decay Widths, Shapes, and Production Amplitudes* *Phys. Rev. D* **5** (624–638) (1972)
- [15] Zemach, C. *Use of angular momentum tensors* *Phys.Rev.* **140** (B97-B108) (1965)
- [16] Rarita, W., Schwinger, J. *On a theory of particles with half integral spin* *Phys.Rev.* **60** (61) (1941)
- [17] Chung, S. U. *General formulation of covariant helicity-coupling amplitudes* *Phys. Rev. D* **57** (431-442) (1998)
- [18] Tibshirani, R. *Regression Shrinkage and Selection Via the Lasso* *Journal of the Royal Statistical Society, Series B* **58** (267–288) (1994)
- [19] Baptiste, G., Hardin, J., Stevens, J., Williams, M., *Model selection for amplitude analysis* *JINST* **10** (P09002) (2015)
- [20] BaBar Collaboration *Measurements of CP-Violating Asymmetries in $B^0 \rightarrow a_1^\pm(1260)\pi^\mp$ decays* *Phys. Rev. Lett.* **98** (181803) (2007)
- [21] Belle Collaboration *Measurement of Branching Fraction and First Evidence of CP Violation in $B^0 \rightarrow a_1^\pm(1260)\pi^\mp$ Decays* *Phys. Rev.* **D86** (092012) (2012)
- [22] LHCb Collaboration *Observation of the resonant character of the $Z(4430)^-$ state* *Phys. Rev. Lett.* **112** (222002) (2014)